Evaluation of three semi-empirical approaches to estimate the net radiation over a drip-irrigated olive orchard

ARTICLE *in* CHILEAN JOURNAL OF AGRICULTURAL RESEARCH · SEPTEMBER 2015

Impact Factor: 0.7

4 AUTHORS, INCLUDING:

Samuel Ortega-Farias

Universidad de Talca

92 PUBLICATIONS **385** CITATIONS

SEE PROFILE

Héctor Valdés-Gómez

Universidad de Talca

35 PUBLICATIONS **78** CITATIONS

SEE PROFILE

Evaluation of three semi-empirical approaches to estimate the net radiation over a drip-irrigated olive orchard

Rafael López-Olivari[1], Samuel Ortega-Farías[2*], Luis Morales[3] and Héctor Valdés[2]

ABSTRACT

A study was carried out to calibrate and evaluate three semi-empirical approaches to estimate net radiation (R_n) over a drip-irrigated olive orchard during 2009/10 and 2010/11 seasons. The orchard was planted in 2005 at high density in the Pencahue Valley, Región del Maule, Chile (35º 23' LS; 71º 44' LW; 96 m above sea level). The evaluated models were calculated using the balance between long and short wave radiation. To achieve this objective it was assumed that $T_s = T_a$ for *Model 1*, $T_s = T_{cv}$ for *Model 2* and $T_s = T_r$ for *Model 3* (where T_s = surface temperature; T_a = air temperature; and T_{cv} = temperature inside of the tree canopy; T_r = radiometric temperature). For the three models, the Brutsaert's empirical coefficient (ϕ) was calibrated using incoming long wave radiation equation with the database of 2009/10 season. Thus, the calibration indicated that ϕ was equal to 1.75. Using the database from 2010/11 season, the validation indicated that the three models were able to predict the R_n at a 30-min interval with errors lower than 6%, root mean square error (RMSE) between 26-39 W m^{-2} and mean absolute error (MAE) between 20-31 W m^{-2}. On daily time intervals, validation indicated that models presented errors, RMSE and MAE between 2-3%, 1.22-1.54 MJ m^{-2} d^{-1} and 1.04-1.35 MJ m^{-2} d^{-1}, respectively. The performance of the three R_n-*Models* would be used according to the availability of data to estimate net radiation over a drip-irrigated olive orchard planted at high density.

Key words: actual evapotranspiration, training system, air emissivity, Brutsaert's equation.

INTRODUCTION

Water availability for irrigation has been reduced globally due to frequent drought and competition for water resources among agriculture-industry and urban areas (van de Geijn and Goudriaan 1996;

[1]Instituto de Investigaciones Agropecuarias, INIA Carillanca, km 10 camino Cajón-Vilcún s/n, Temuco, Chile.

[2]Universidad de Talca, Facultad de Ciencias Agrarias, Centro de Investigación y Transferencia en Riego y Agroclimatología, Av. Lircay s/n, Talca, Chile. [*]Corresponding author (sortega@utalca.cl).

[3]Universidad de Chile, Facultad de Ciencias Agronómicas, Santa Rosa, 11315, Santiago, Chile.

Basso et al., 2001). Chile has been periodically affected by El Niño-Southern Oscillation (ENSO) phenomena, which has produced important droughts ("La Niña" event) with associated economical losses in most of agricultural areas (Antonioletti et al., 2002). Under these conditions, it is required a better irrigation water management to optimize water efficiency of cultivated plants. For this purpose, it is critical the accurate determination of actual evapotranspiration (ET_a). For fruit orchards, ET_a is calculated using a reference evapotranspiration (ET_o) from a grass or alfalfa-surface multiplied by specific crop-coefficients (K_c). Furthermore, several researchers have suggested using three or two-source models to directly compute ET_a. These models are based on the Penman-Monteith approach to compute separately plant transpiration from soil evaporation (Shuttleworth and Wallace, 1985; Brenner and Incoll, 1997; Domingo et al., 1999; Testi et al., 2006; Ortega-Farías et al., 2007; Were et al., 2008; Zhang et al., 2008; Poblete-Echeverría and Ortega-Farías, 2009; Ortega-Farías and López-Olivari, 2012). The use of ET_a models requires an appropriate parameterization of the available energy, where the net radiation (R_n) is the most important factor.

In general, the R_n has been estimated using empirical models or linear regressions, which use the incident solar radiation as the main input variable (Fritschen, 1967; Kustas et al., 1994; Al-Riahi et al., 2003; Alados et al., 2003; Almeida and Landsberg, 2003). Pereira et al. (2007) used a simple approach to transform daily values of grass R_n into whole tree canopy net radiation for walnut, apples, olives and citrus. However, these models are site-specific and do not consider the long wave components in the calculation of R_n. On the other hand, there are semi-empirical models based on Stefan-Boltzmann law that includes the estimation of long wave radiation into the R_n formulation. The accuracy of these models depends mainly on the atmospheric emissivity (ε_a) for which there are several ways of calculations in literature (Anderson, 1954; Swinbank, 1963; Idso and Jackson, 1969; Idso, 1981; Bastiaanssen, 1995; Prata, 1996), but many of them are empirical and generally site-specific. Among the semi-empirical algorithms to calculate ε_a we can highlight the Brutsaert's equation, which is based on radiative transfer theory. For agricultural applications, the Brutsaert's emissivity equation has been widely used to compute R_n for several crops such as green grass, maize, pecan and cottonwood trees and grapevines (Allen et al., 1998; Ortega-Farías et al., 2000; Samani et al., 2007; Carrasco and Ortega-Farías, 2008; Irmak et al., 2010). Recently, Ezzahar et al. (2007) used the original Brutsaert's equation to estimate long-wave radiation for an irrigated olive orchard. In this study, the authors used as input the surface temperature computed as a function of soil and canopy temperatures, and fractional cover. Furthermore, Berni et al. (2009) used the same equation incorporating the cloud fraction term (*clf*) to correct the emissivity on clear conditions for

a drip-irrigated olive orchard. The empirical coefficient (ϕ) of the Brutsaert's equation depends on variations of climate characteristics, thus a local calibration of ϕ is required to improve the calculation of R_n (Sugita and Brutsaert, 1993).

In literature there are few semi-empirical methods to estimate R_n over fruit trees especially for olive orchard planted at high density (> 1,300 trees ha^{-1}). In this regard, the objective of this research was to evaluate three semi-empirical models to estimate net radiation (R_n) over a drip-irrigated olive orchard planted at high density.

Net radiation model

Net radiation (R_n) is considered as the sum of incoming and outgoing shortwave and long-wave radiation, which is also a measure of the available energy at an underlying surface. It is also considered the fundamental parameter that commands the climate of the planetary boundary layer, being the driving force for processes, such as, evapotranspiration, air and soil heating, and photosynthesis. The daytime variation of net radiation over an olive orchard can be calculated as:

$$R_{ne} = (1-\alpha)R^{\downarrow} + \left(R_l^{\downarrow} - R_l^{\uparrow}\right) \quad (1)$$

$$R_{ne} = (1-\alpha)R^{\downarrow} + \sigma\left(\varepsilon_a T_a^{\,4} - \varepsilon_s T_s^{\,4}\right) \quad (2)$$

where, R_{ne} = estimated net radiation (W m^{-2}); $R^{\downarrow}$ = incoming short wave solar radiation (W m^{-2}); $R_l^{\downarrow}$ = incoming long wave solar radiation (W m^{-2}); $R_l^{\uparrow}$ = outgoing long wave solar radiation (W m^{-2}); α = albedo (dimensionless); ε_s = surface emissivity (dimensionless); ε_a = atmospheric emissivity (dimensionless); T_a = air temperature (K); T_s = surface temperature (K); σ = Stefan-Boltzmann constant (5.67x10^{-8} W m^{-2} K^{-4}). ε_a is determined according to the following expression (Brutsaert, 1975):

$$\varepsilon_a = \phi(e_a / T_a)^{1/7} \quad (3)$$

$$e_a = e_s RH / 100 \quad (4)$$

where, e_a = air vapour pressure (kPa); RH = relative humidity (%); e_s = saturated vapour pressure (kPa); ϕ = empirical coefficient.

MATERIALS AND METHODS

General description

The experiment was conducted during the 2009/10 and 2010/11 growing seasons on a drip-irrigated olive orchard (*Olea europaea* L. cv Arbequina) for oil production. The orchard had an extension of 2.7 hectares is located in the Pencahue Valley, Maule Region, Chile (35º 23' LS; 71º 44' LW; 96 m above sea level) with a slope of 1.6 %. The olive trees were planted in 2005 in east-west orientated rows. Trees were planted 5m apart with 1.5m within-row (1,333 trees per hectare) and conducted in cone trellis system at a height of 3.2 m and canopy width of 1.55 m. The climate in this area is a typical Mediterranean semiarid climate with a daily average temperature of 14.8 °C between September and May. Average annual rainfall in the region reaches 602 mm mainly concentrated during the winter months (June-September). The summer period is usually dry (3.5 % of annual rainfall) and hot with high atmospheric demand for water vapour. The soil is classified as the Quepo series (Vertisol, Family Fine, thermic Xeric Apiaquerts) with a clay loam texture (CIREN, 1997).

Meteorological measurements

An automatic weather station was installed to measure meteorological variables over a drip-irrigated olive orchard planted at high density. Wind speed (u) and wind direction (w) were monitored by a cup anemometer and a wind vane (03101-5, Young, Michigan, USA), respectively. Precipitation (Pp) was measured by a rain gauge (A730RAIN, Adcon Telemetry, Austria). Air temperature (T_a) and air relative humidity (RH_a) were measured using HOBO Pro RH/Temp sensors (Onset Computer, Inc., Bourne, Massachusetts, USA). Net radiation (R_n), incoming ($R^{\downarrow}$) and outgoing ($R^{\uparrow}$) solar radiation were measured by a four-way net radiometer (CNR1, Kipp&Zonen Inc., Delft, Netherlands) installed at 1.9 m above the tree canopy. In this radiometer, the short and long wave solar radiations are measured by two CM3 pyranometers and two CG3 pyrgeometers, respectively. Half-hour averages of all balance radiation signals were recorded on an electronic datalogger (CR5000, Campbell Sci, Logan, UT). Sensors of u, w, Pp, T_a and RH_a were installed at 4.8 m above the soil surface. Also, a HOBO sensor to measure canopy temperature (T_{cv}) and relative humidity (RH_{cv}) was installed inside the canopy at 1.5 m above the soil surface.

Finally, a hand-held multi-spectral radiometer equipped with sun angle cosine correction capacity (MSR16R, CropScan Inc., Rochester, MN) was used to estimate the Normalized Difference Vegetation Index (NDVI) over the canopy and soil surface between rows. The measures of multi-

spectral radiometer were recorded once a week. The multi-spectral radiometer was manually transported and a support pole was used to position the radiometer 0.5 m above the tree canopy.

Irrigation management and soil-plant measurements

Irrigation water was delivered four times per week using 2.1 L h^{-1} drippers spaced at 0.75 m intervals along the rows (two drippers per plant). Olive tree water status was evaluated, every fifteen days, using midday stem water potential (ψ_x) measured with a pressure chamber (model 1000, PMS Instrument Co., Corvallis, Oregon, USA) on 30 shoots (one shoot per tree) covered for 2 h before measurement with a plastic bag and aluminium foil. Olive trees were maintained under *non-water-stress conditions* (ψ_x > -1.5 MPa) during both studied seasons (Moriana et al., 2007; Gómez-del-Campo et al., 2008). The fractional cover (f_c) of the olive orchard was calculated according to Er-Raki et al. (2008) methodology obtaining values of 0.29 (±0.07) and 0.30 (±0.05) for the 2009/10 and 2010/11 seasons, respectively. Two averaging thermocouples probes (TCAV, Campbell Sci., Logan, UT) were used to measure soil temperature (T_{soil}) installed at 0.02 and 0.06 m of depth (two pairs in the inter row and two pairs below the row). Averages of 30-min for all thermocouples probes were recorded using an electronic datalogger (CR3000, Campbell Sci, Logan, UT).

Calibration and evaluation

The calibration of the original Brutsaert's coefficient (ϕ=1.24) was carried out using a database (T_a, RH, $R_l^{\uparrow}$) from December 2009 to February 2010. At 30-min interval, the calibrated value of ϕ was obtained using the following equation:

$$R_l^{\downarrow} = \phi (e_a / T_a)^{1/7} \sigma T_a^4 \qquad (5)$$

The model evaluation was done using data collected from December 2010 to February 2011. In this case, the following three approaches were used to calculate daytime variation of R_{ne}:

a) Assuming that $T_s = T_a$, equation (2) becomes (***Model 1***):

$$R_{ne} = (1-\alpha)R^{\downarrow} + \sigma T_a^4 \left(\phi \left(\frac{e_a}{T_a} \right)^{\frac{1}{7}} - \varepsilon_s \right) \qquad (6)$$

b) Assuming that $T_s = T_{cv}$, equation (2) becomes (***Model 2***):

$$R_{ne} = (1-\alpha)R^{\downarrow} + \sigma\left(\phi\left(\frac{e_a}{T_a}\right)^{\frac{1}{7}} T_a^4 - \varepsilon_s T_{cv}^4\right) \quad (7)$$

c) Assuming that $T_s = T_r$, equation (2) becomes (***Model 3***):

$$R_{ne} = (1-\alpha)R^{\downarrow} + \sigma\left(\phi\left(\frac{e_a}{T_a}\right)^{\frac{1}{7}} T_a^4 - \varepsilon_s T_r^4\right) \quad (8)$$

In the last model, T_r correspond to the radiometric temperature which was estimated as follow: (Norman et al., 1995; Ezzahar et al., 2007; Morillas et al., 2013):

$$T_r \approx C\sqrt[4]{f_c T_{cv}^{\ 4} + (1 \quad f_c) T_{soil}^{\ 4}} \quad (9)$$

where T_{soil} and T_{cv} are soil and canopy temperatures (K), respectively. f_c is the fractional cover of the olive orchard (0.29 and 0.30 during 2009/10 and 2010/11 seasons, respectively) and C is the empirical coefficient (C = 0.85).

The surface emissivity was calculated as follow (Morales, 1997):

$$\varepsilon_s = 0.9585 + 0.0357\left(NDVI_{avg}\right) \quad (10)$$

where $NDVI_{avg}$ is the average Normalized Difference Vegetation Index. The values of $NDVI_{avg}$ were computed as:

$$NDVI_{avg} = \frac{\sum_{i=1}^{m}\left(f_c NDVI_r + (1-f_c) NDVI_{br}\right)}{n} \quad (11)$$

where $NDVI_{br}$ is the normalized difference vegetation index measured from soil between rows (dimensionless); $NDVI_r$ is the normalized vegetation index measured above olive canopy (dimensionless); n is the number of total measurements and m is the individual measurement.

Statistical analysis

For calibration, estimated values of $R_l^{\downarrow}$ were compared to those measured by a CG3 pyrgeometer including the root mean square error (RMSE) and mean absolute error (MAE). For the validation, estimated values of net radiation (R_{ne}) using *Models 1*, *2* and *3* were compared to those measured by CNR1. Daily and 30-min comparisons included the R_{ne}/R_n (r_{eo}) and $R_{el}^{\downarrow}/R_l^{\downarrow}$ (r_{eol}) ratios, RMSE, MAE and index of agreement (I_a) (Willmott, 1981; Mayer and Butler, 1993). Additionally, the Z-test was used to check whether the value of r_{eo} was significantly different from unity at the 95% confidence level.

RESULTS

Climatic conditions

Daily mean values of incoming short wave radiation ($R^{\downarrow}$) were between 2.4-33.9 and 4.5-34.2 MJ m^{-2} d^{-1} for the 2009/10 and 2010/11 season, respectively. Daily mean values of measured net radiation (R_n) ranged between 0.2-21.9 MJ m^{-2} d^{-1} for 2009/10 season and 3.5-21.8 MJ m^{-2} d^{-1} for 2010/11 season (Figure 1a and d). The ratio of R_n to $R^{\downarrow}$ were about 0.46 and 0.62 during the first and second seasons, respectively. The average (T_{avg}), maximum (T_{max}) and minimum (T_{min}) air temperatures throughout 2009/10 season were 17.9, 27.9 and 9.1 °C, respectively (Figure 1b). Temperatures during 2010/11 season were of 19.4, 29.2 and 10.4 °C for T_{avg}, T_{max} and T_{min}, respectively (Figure 1e). The values of minimum air temperature during the period of measurements throughout 2009/10 and 2010/11 seasons were of 6.2 and 4.1°C, respectively, while those of maximum air temperature during 2009/10 and 2010/11 seasons were 35.7 and 38.3°C, respectively. For the 2009/10 season, mean values of D_{avg}, D_{max} and D_{min} were 1.1, 2.8 and 0.11 kPa, respectively (Figure 1c), while those observed during 2010/11 season were of 1.2, 3.0 and 0.10 kPa, respectively (Figure 1f**)**.

Calibration model

For the 2009/10 database, the Brutsaert's coefficient was of ϕ = 1.75 for all three models using a non-linear optimization. In this case, the $R_l^{\downarrow}$ values were underestimated by about 1 and 30% for ϕ equal to 1.75 and 1.24, respectively. Also, RMSE and MAE values were 22 and 17 W m^{-2} for ϕ = 1.75 while those were 101 and 98 W m^{-2} for ϕ = 1.24, respectively (Table 1). For ϕ = 1.75, the $R_{el}^{\downarrow}$ /

$R_l^{\downarrow}$ ratio (r_{eol}) and index of agreement (I_a) were more close to 1, with values of 0.99 and 0.84, respectively. However, for ϕ = 1.24, the r_{eol} and I_a indexes were 0.70 and 0.28, respectively (Table 1). Crawford and Duchon (1999) suggested seasonal adjustments to the ϕ coefficient ranging from 1.28 in January to 1.16 in July (North Hemisphere). Sridhar and Elliott (2002) for Oklahoma and Culf and Gash (1993) for Niger found a mean value of 1.31 to four different geographic and climatic conditions. However, Sugita and Brutsaert (1993) suggested a new empirical coefficient of 0.98 using data from the First International Satellite Land Surface Climatology Project (ISLSCP) Field Experiment (FIFE). In this regard, Sugita and Brutsaert (1993) proposed to locally calibrate the Brutsaert's formula in order to accurately estimate the incoming long wave radiation for specific agroclimatic conditions. Sicart et al. (2010) indicated that the ϕ values depend directly on local atmospheric conditions where changes in temperature and humidity certainly are the main factors.

For the 2009/10 database, the comparison between measured and computed R_n indicated that *Models 1*, *2* and *3* using ϕ = 1.75 presented errors between 4-5%, whereas those using ϕ = 1.24 had errors between 10-11%. In this regard, Brotzge and Deuchon (2000) and Brotzge and Crawford (2003) reported that the possible errors in the estimation of R_n for cloudy days could be associated with the parameterization of the air emissivity. Furthermore, Ezzahar et al. (2007) and Ortega-Farías et al. (2000) showed that the use of the uncalibrated Brutsaert's formula that might create an important scattering for low R_n values. For all-sky condition, the major difficulty was associated with the estimation of the long wave radiation, which it is related to the surface temperature (T_s).

Model Evaluation

The mean albedo value (α) obtained using measurements of $R^{\uparrow}/R^{\downarrow}$ ratios from 09:00 to 18:00 hours is indicated in the Figure 2, which indicates that the albedo was relatively stable and ranged between 0.15-0.18 for clear and cloudy day. Thus, a mean albedo equal to 0.17 (± 0.015) was used for the models evaluation using the 2010/11 database. A similar albedo (α = 0.17) was observed by Cammalleri et al. (2010) for an olive orchard with a canopy height and fractional cover equal to 3.7 m and 0.35, respectively.

A good agreement was obtained between measured (R_n) and estimated (R_{ne}) values of net radiation for the three models during the 2010/11 database (Table 2). Using data at 30-min time interval, the model evaluation indicated that RMSE was between 26-39 W m^{-2} and MAE was between 21-31 W m^{-2} for the three models. The Z-test showed that r_{eo} was significantly different from unity suggesting that the three models tended to overestimated R_n with an error lower than 6% (Table 2).

For the daily comparison, the Table 2 indicates that the *Model 3* presented the highest values of RMSE (39 W m^{-2}) and MAE (31 W m^{-2}). Furthermore, the Z-test shows that r_{eo} was significantly different from unity indicating that the *Models 1*, *2* and *3* overestimated R_n with errors lower than 3% (Table 2). Finally, the index of agreement (I_a) on 30 min time interval were close to 1.0 while those on daily basis ranged between 0.93-0.96.

The comparisons between observed and estimated values of R_n on 30 min intervals and daily basis are shown in the Figure 3. This Figure indicates that the points were close to the 1:1 line, but at 30-min time intervals the three models tended to overestimate and underestimate the observed R_n for values > 600 W m^{-2} and R_n < 200 W m^{-2}, respectively (Figure 3a, c and e). On daily intervals, the *Models 1*, *2* and *3* overestimated observed R_n for values between 17 and 20 MJ m^{-2} d^{-1} (Figure 3b, d and f).

The daytime variation of observed and estimated R_n for the best and worse comparisons is presented in Figure 4. For clear sky conditions, the best comparison was observed on DOY 17, which presented the maximum differences at noon, with values of -40, -37 and -66 W m^{-2} for the *Models 1*, *2* and *3*, respectively. During night-time, maximum differences were 30, 26 and 37 W m^{-2} for *Models 1*, *2* and *3*, respectively (Figure 4a). The worse performance on clear days were observed on DOY 5 where the maximum differences were -55, -54 and -82 W m^{-2} for *Models 1*, *2* and *3*, respectively. During night-time, the *Models 1*, *2* and *3* presented maximum differences ranging between 30 and 40 W m^{-2} (Figure 4b). For cloudy days, the best comparison was observed in DOY 337 where the maximum differences between R_n and R_{ne} during daytime were between -23 and -43 W m^{-2} while those during night-time were between 22 and 39 W m^{-2} for the three evaluated models (Figure 4c). For cloudy sky conditions, the worse comparison during the daytime was observed on DOY 16 where the maximum differences ranged between -103 and 102 W m^{-2} for the three models. During night-time, the *Models 1*, *2* and *3* presented maximum differences of 52, 51 and 77 W m^{-2}, respectively (Figure 4d).

DISCUSSIONS

Results obtained in this research agree to those observed in the literature for grass, tree orchards, vineyards, and maize. For a drip-irrigated Cabernet sauvignon vineyard (f_c = 0.30), Carrasco and Ortega-Farías (2008) indicated that equation 16 (see Table 3) underestimated the observed values of R_n at 30-min time interval with an error and RMSE of 6% and 45 W m^{-2}, respectively. On daily basis, equation 16 underestimate the R_n with an error of 5% and a RMSE of 1.21 MJ m^{-2} d^{-1}. For a

drip-irrigated Merlot vineyard (f_c = 0.30), Ortega-Farías et al. (2010) found that equation 22 underestimated the observed values of daily R_n with an error equal to 6% and a RMSE of 1.3 MJ m^{-2} d^{-1}. For olive orchards, Berni et al. (2009) reported a good fit between R_{ne} and R_n with a RMSE equal to 23 W m^{-2} (Equation 18) for clear sky condition, whereas Ezzahar et al. (2009) observed an underestimate equal to 7% with a root mean square difference (RMSD) of about 60 W m^{-2} (Equation 19). Samani et al. (2007) tested an R_n-model (Equation 15) observing a standard error of estimate (SEE) for the daily R_n of 1.65 MJ m^{-2} d^{-1} for Pecan tree; 1.06 MJ m^{-2} d^{-1} for Saltcedar tree and 1.17 MJ m^{-2} d^{-1} for Cottonwood tree. Kjaersgaard et al. (2009) tested an R_n-model (Equation 20) on a field covered with green grass (Denmark) observing a RMSE and MAE of 1.47 and 1.22 MJ m^{-2} d^{-1}, respectively. Irmak et al. (2003) using the FAO56-R_n model (Equation 13) observed a mean standard error equal to 1.24 MJ m^{-2} d^{-1} for four locations in USA. They also proposed, for the same locations, a polynomial equation (Equation 14) to estimate R_n obtaining a mean standard error of 1.18 MJ m^{-2} d^{-1}. For grass at reference condition, Ortega-Farías et al. (2000) observed that equation 12 simulated the hourly R_n for Avignon (France) and in Talca (Chile) with a RMSE of 34 and 42 W m^{-2}, respectively. For a turfgrass field, Sentelhas and Gillespie (2008) in Canada (Eloria, Ontario) used an empirical R_n-model (Equation 17), parameterized by Iziomon et al. (2000), obtaining a MAE of about 28 W m^{-2}. For maize crop (Nebraska and California, USA), Irmak et al. (2010) reported that the ASCE-EWRI R_n-model (Equation 21) predicted daily R_n with a RMSD of 1.44 MJ m^{-2} d^{-1} and an error of 7%. In summary, the validation of the three approaches indicated that the ranges of statistical parameters are similar to those found in other model validations (Table 3).

In general, the three evaluated approaches presented a good performance to estimate R_n for the different assumptions showed here. It is important to acknowledge that the parameterization of R_n, depend on the training system, canopy arquitecture, plant density and fractional cover (Ortega-Farías et al., 2010). In this study, a constant shape of the canopy was maintained with f_c ranging between 0.29-0.30 during the two growing seasons (calibration and validation model). Under this constant shape, the daily ratios of $R^{\uparrow}$ to $R^{\downarrow}$ were quite constant ($\alpha = 0.17 \pm 0.015$), allowing a good performance of the models 1, 2 and 3 during the two study periods.

CONCLUSIONS

At 30-min intervals, the model validation using ϕ = 1.75 and albedo = 0.17 indicated that the three approaches were able to simulate the R_n over a drip-irrigated olive orchard with an RMSE and MAE lower than 39 and 31 W m^{-2}, respectively. On a daily basis, the three models presented a RMSE < 1.54 MJ m^{-2} d^{-1} and MAE < 1.35 MJ m^{-2} d^{-1}. Furthermore, the three semi-empirical models showed

errors lower than 6 and 3% for a 30-minute and daily time intervals, respectively. Finally, the three R_n-*Models* presented here would be used depending of the availability of data. Future research will be centered on the effect of the training system on the parameterization of R_n. Also, we will explore the application of remote sensing to simulate the ground surface area cover which depends on olive tree vigor and canopy geometry.

ACKNOWLEDGEMENTS

The research leading of this research was supported by The Chilean Government through the projects "Comisión Nacional de Riego" (CNR), FONDEF (Nº D10I1157), FONDECYT N°1100714 and Universidad de Talca through the research program "Adaptation of Agriculture to Climate Change (A2C2).

LITERATURE CITED

Alados, I., I. Foyo-Moreno, F.J. Olmo, and L. Alados-Arboledas 2003. Relationship between net radiation and solar radiation for semi-arid shrub-land. Agricultural and Forest Meteorology 116:221–227.

Allen, R.G., L.S. Pereira, D. Raes, and M. Smith 1998. Crop evapotranspiration. Guidelines for computing crop water requirement. FAO Irrigation and Drainage Paper Nº 56. 300 p. FAO, Rome, Italy.

Almeida, A.C., and J.J. Landsberg 2003. Evaluating methods of estimating global radiation and vapour pressure deficit using a dense network of automatic weather stations in coastal Brazil. Agricultural and Forest Meteorology 118:237–250.

Al-Riahi, M., K. Al-Jumaily, and I. Kamies 2003. Measurements of net radiation and its components in semi-arid climate of Baghdad. Energy Conversion and Management 44:509–525.

Anderson, E.R. 1954. Energy budget studies, Water loss investigations: Lake Hefner Studies. Technical report. U.S. Geological Survey Professional Paper N° 269, 71-119.

Antonioletti, R., P. González, S. Ortega-Farías 2002. Caractérisation des événements El Niño par des variables climatiques et leur impact sur l"activité agricole au Chili central. Climat et environnement, L' information climatique au service de la gestion de l´environnement, Publications de l´Association Internationale de Climatologie. Institut de Géographie – France. 14:105-110.

Basso, E., R. Compagnucci, P. Fearnside, G. Magrin, J. Marengo, A.R. Moreno, A. Suárez, S. Solman, A. Villamizar, and L. Villers 2001. 14 Latin America. In: McCarthy, J.J., O.F.

356 Canziani, N.A. Leary, D.J. Dokken, K.S. White. Climate Change 2001: Impacts, Adaptation, and
357 Vulnerability. Intergovernmental Panel on Climate Change (IPCC), GRID Arendal. 695-724.
358 Bastiaanssen, W.G. 1995. Regionalization of flux densities and moisture indicators in composite
359 terrain: a remote sensing approach under clear skies in Mediterranean climates. Department of
360 Water Resources, Wageningen University, The Netherlands.
361 Berni, J.A.J., P.J. Zarco-Tejada, G. Sepulcre-Cantó, E. Fereres, and F. Villalobos 2009. Mapping
362 canopy conductance and CWSI in olive orchards using high resolution thermal remote sensing
363 imagery. Remote Sensing of Environment 113:2380–2388.
364 Brenner, A.J., and L.D. Incoll 1997. The effect of clumping and stomatal response on evaporation
365 from sparsely vegetated shrublands. Agricultural and Forest Meteorology 84:187-205.
366 Brotzge, J., and K. Crawford 2003. Examination of the surface energy budget: a comparison of
367 eddy correlation and Bowen ratio measurements systems. Journal of Hydrometeorology 4:160–
368 178.
369 Brotzge, J., and C. Deuchon 2000. A field comparison among a domeless net radiometer, two four-
370 component net radiometers, and a domed net radiometer. Journal of Atmospheric and Oceanic
371 Technology 17:1569–1582.
372 Brutsaert, W. 1975. On a derivable formula for longwave radiation from clear skies. Water
373 Resources Research 11: 742–744.
374 Cammalleri, C., C. Agnese, G. Ciraolo, M. Minacapilli, G. Provenzano, and G. Rallo 2010. Actual
375 evapotranspiration assessment by means of a coupled energy/hydrologic balance model:
376 Validation over an olive grove by means of scintillometry and measurements of soil water
377 contents. Journal of Hydrology 392:70-82.
378 Carrasco, M., and S. Ortega-Farías 2008. Evaluation of a model to simulate net radiation over a
379 vineyard cv. Cabernet Sauvignon. Chilean Journal of Agricultural Research 68:156–165.
380 Centro de Investigación de Recursos Naturales (CIREN). 1997. Estudio Agrológico, VII Región.
381 Descripciones de Suelos. Materiales y Símbolos. Centro de Información de Recursos Naturales.
382 Santiago. Publicación N° 117. 659 p.
383 Crawford, T.M., and C.E. Duchon 1999. An improved parameterization for estimating effective
384 atmospheric emissivity for use in calculating daytime downwelling longwave radiation. Journal
385 of Applied Meteorology 38:474–480.
386 Culf, A.D., and J.H.C. Gash 1993. Longwave radiation from clear skies in Niger: a comparison of
387 observations with simple formulas. Journal of Applied Meteorology 32:539–547.

388 Domingo, F., L. Villagarcia, A.J. Brenner, and J. Puigdefabregas 1999. Evapotranspiration model
389 for semi-arid shrub-lands tested against data from SE Spain. Agricultural and Forest
390 Meteorology 95:67-84.
391 Er-Raki, S., A. Chehbouni, J. Hoedjes, J. Ezzahar, B. Duchemin, and F. Jacob 2008. Improvement
392 of FAO-56 method for olive orchards through sequential assimilation of thermal infrared-based
393 estimates of ET. Agricultural Water Management 95:309-321.
394 Ezzahar, J., A. Chehbouni, J. Hoedjes, D. Ramier, N. Boulain, S. Boubkraoui, B. Cappelaere, L.
395 Descroix, B. Mougenot, and F. Timouk 2009. Combining scintillometer measurements and an
396 aggregation scheme to estimate area-averaged latent heat flux during the AMMA experiment.
397 Journal of Hydrology 375: 217–226.
398 Ezzahar, J., A. Chehbouni, J.C.B. Hoedjes, S. Er-Raki, A.H. Chebouni, G. Boulet, J.M. Bonnefond,
399 and H.A.R. Bruin 2007. The use of the scintillation technique for monitoring seasonal water
400 consumption of olive orchards in a semi-arid region. Agricultural Water Management 89:173–
401 184.
402 Fritschen, L.J. 1967. Net and solar radiation relations over irrigated field crops. Agricultural
403 Meteorology 4:55–62.
404 Gómez-del-Campo, M., A. Leal García, and C. Pezuela Espliego 2008. Relationship of stem water
405 potential and leaf conductance to vegetative growth of young olive trees in a hedgerow orchard.
406 Australian Journal of Experimental Agriculture 59(3):270 – 279.
407 Idso, S.B. 1981. A set of equations for full spectrum and 8- to 14-μm and 10.5- to 12.5-μm thermal
408 radiation from cloudless skies. Water Resources Research 17(2):295-304.
409 Idso, S.B., and R.D. Jackson 1969. Thermal radiation from the atmosphere. Journal of Geophysical
410 Research 74:3397-3403.
411 Irmak, S., A. Irmak, J.W. Jones, T.A. Howell, J.M. Jacobs, R.G. Allen, and G. Hoogenboom 2003.
412 Predicting Daily Net Radiation Using Minimum Climatological Data. Journal of Irrigation and
413 Drainage Engineering 129(4):256-269.
414 Irmak, S., D. Mutiibwa, and O. Payero 2010. Net Radiation Dynamics: Performance of 20 Daily
415 Net Radiation Models as Related to Model Structure and Intricacy in Two Climates.
416 Transactions of the ASABE 53(4):1059-1076.
417 Iziomon, M.G., H. Mayer, and A. Matzarakis 2000. Empirical models for estimating net radiation
418 flux: a case study for three mid-latitude sites with orographic variability. Astrophysics and Space
419 Science 273: 313–330.

420 Kjaersgaard, J.H., R.H. Cuenca, A. Martínez-Cob, P. Gavilán, F. Plauborg, M. Mollerup, and S.
421 Hansen 2009. Comparison of the performance of net radiation calculations models. Theoretical
422 and Applied Climatology 98:57-66.
423 Kustas, W.P., R.T. Pinker, T.J. Schmugger, and K.S. Humes 1994. Net radiation estimated for
424 semiarid rangeland basin sensed date. Agricultural and Forest Meteorology 71:337–357.
425 Mayer, D.G., and D.G. Butler 1993. Statistical validation. Ecological Modelling 68:21-31.
426 Morales, S.L. 1997. Evaluación y zonificación de riesgo de heladas mediante modelización
427 topoclimática. Tesis Doctoral Ciencias Ambientales. Universidad de Concepción, Chile. 143 p.
428 Moriana, A., D. Pérez-López, A. Gómez-Rico, M.D. Salvador, N. Olmedilla, F. Ribas, and G.
429 Fregapane 2007. Irrigation scheduling for traditional, low-density olive orchards: Water relations
430 and influence on oil characteristics. Agricultural Water Management 87:171–179.
431 Morillas, L., M. García, H. Nieto, L. Villagarcia, I. Sandholt, M.P. Gonzalez-Dugo, P.J. Zarco-
432 Tejada, and F. Domingo 2013. Using radiometric surface temperature for surface energy flux
433 estimation in Mediterranean drylands from a two-source perspective. Remote Sensing of
434 Environment 136: 234–246.
435 Norman, J.M., W.P. Kustas, and K.S. Humes 1995. A two-source approach for estimating soil and
436 vegetation energy fluxes from observations of directional radiometric surface temperature.
437 Agricultural and Forest Meteorology 77:263–293.
438 Ortega-Farías, S., R. Antonioletti, and A. Olioso 2000. Net radiation model evaluation at an hourly
439 time step for Mediterranean conditions. Agronomie 20(1):157-164 (INRA-Francia).
440 Ortega-Farías, S., M. Carrasco, A. Olioso, C. Acevedo, and C. Poblete 2007. Latent heat flux over a
441 Cabernet Sauvignon vineyard using the Shuttleworth and Wallace model. Irrigation Science
442 25:161-170.
443 Ortega-Farías, S., C. Poblete-Echeverria, and N. Brisson 2010. Parameterization of a two-layer
444 model for estimating vineyard evapotranspiration using meteorological measurements.
445 Agricultural Water Management 150:276–286.
446 Ortega-Farías, S., and R. López-Olivari 2012. Validation of a two-layer model to estimate latent
447 heat flux and evapotranspiration in a drip-irrigated olive orchard. Transactions of the ASABE
448 55(4):1169-1178.
449 Pereira, A.P., S. Green, and N.A. Villa Nova 2007. Relationships between single tree canopy and
450 grass net radiations. Agricultural and Forest Meteorology 142:45–49.
451 Poblete-Echeverría, C., and S. Ortega-Farías 2009. Estimation of actual evapotranspiration for a
452 drip-irrigated Merlot vineyard using a three-source model. Irrigation Science 28:65–78.

453 Prata, A.J. 1996. A new long-wave formula for estimating downward clear-sky radiation at the
454 surface. Quarterly Journal of the Royal Meteorological Society 122:1127-1151.
455 Samani, Z., A.S. Bawazir, M. Bleiweiss, R. Skaggs, and V.D. Tran 2007. Estimating Daily Net
456 Radiation over Vegetation Canopy through Remote Sensing and Climatic Data. Journal of
457 Irrigation and Drainage Engineering 133(4):291-297.
458 Sentelhas, P.C., and T.J. Gillespie 2008. Estimating hourly net radiation for leaf wetness duration
459 using the Penman-Monteith equation. Theoretical and Applied Climatology 91:205–215.
460 Shuttleworth, W.J., and J.S. Wallace 1985. Evaporation from sparse crops-an energy combination
461 theory. Quarterly Journal of the Royal Meteorological Society 111:839-855.
462 Sicart, J.E., R. Hock, P. Ribstein, J.P. Chazarin 2010. Sky long-wave radiation on tropical Andean
463 glaciers: Parameterization and sensitivity to atmospheric variables. Journal of Glaciology
464 56(199): 854–860.
465 Sridhar, V., and R.L. Elliott 2002. On the development of a simple downwelling longwave radiation
466 scheme. Agricultural and Forest Meteorology 112:237–243.
467 Sugita, M., and W. Brutsaert 1993. Cloud effect in the estimation of instantaneous downward
468 longwave radiation. Water Resources Research 29 (3):599–605.
469 Swinbank, W.C. 1963. Long-wave radiation from clear skies. Quarterly Journal of the Royal
470 Meteorological Society 89:339-348.
471 Testi, L., F.J. Villalobos, F. Orgaz, and E. Fereres 2006. Water requirements of olive orchards: I
472 simulation of daily evapotranspiration for scenario analysis. Irrigation Science 24:69-76.
473 van de Geijn, S., and J. Goudriaan 1996. The effects of elevated CO2 and temperature change on
474 transpiration and crop water use. In: Bazzaz, F., and W. Sombroek. Global climate change and
475 agricultural production. FAO y John Wiley & Sons Ltd. Roma, Italia. 358 p.
476 Were, A., L. Villagarcia, F. Domingo, M.J. Moro, and A.J. Dolman 2008. Aggregating spatial
477 heterogeneity in a bush vegetation patch in semi-arid SE Spain: A multi-layer model versus a
478 single-layer model. Journal of Hydrology 349:156-167.
479 Willmott, C.J. 1981. On the validation of models. Physical Geography 2:184–194.
480 Zhang, B., S. Kang, F. Li, and L. Zhang 2008. Comparison of three evapotranspiration models to
481 Bowen ratio-energy balance method for a vineyard in a desert region of northwest China.
482 Agricultural and Forest Meteorology 148:1629-1640.
483
484 **Tables and Figures**
485 **Table 1. Statistical evaluation for three semi-empirical models to estimate incoming long wave**
486 **radiation ($R_l^{\downarrow}$) and net radiation (R_n) over a drip-irrigated olive orchard planted at high**
487 **density during the 2009/10 season.**

30-min comparison	Number of observations	RMSE (W m^{-2})	MAE (W m^{-2})	I_a	$r_{eo} = R_{ne} / R_n$ $r_{eol} = R_{el}^{\downarrow} / R_l^{\downarrow}$	Z-test
Estimated $R_l^{\downarrow}$ (ϕ = 1.75)	1,200	22	17	0.84	0.99	F
Estimated $R_l^{\downarrow}$ (ϕ = 1.24)	1,200	101	98	0.28	0.70	F
Model 1 (ϕ = 1.75)	1,200	27	22	1.00	1.05	F
Model 1 (ϕ = 1.24)	1,200	93	90	0.98	0.89	F
Model 2 (ϕ = 1.75)	1,200	26	21	1.00	1.04	F
Model 2 (ϕ = 1.24)	1,200	93	90	0.98	0.89	F
Model 3 (ϕ = 1.75) (C = 0.85)	1,200	31	25	1.00	1.05	F
Model 3 (ϕ = 1.24) (C = 0.85)	1,200	101	97	0.97	0.90	F

RMSE = root mean square error; MAE = mean absolute error; I_a = index of agreement; r_{eo} = ratio of estimated (R_{ne}) to observed (R_n) values of net radiation on 30-min; r_{eol} = ratio of estimated ($R_{el}^{\downarrow}$) to observed ($R_l^{\downarrow}$) values of incoming long wave radiation on 30-min; T = true hypothesis ($b = 1$); F = false hypothesis ($b \neq 1$).

Table 2. Statistical evaluation for three semi-empirical models to estimate net radiation (R_n) over a drip-irrigated olive orchard planted at high density during the 2010/11 season.

30-min comparison	Number of observations	RMSE (W m^{-2})	MAE (W m^{-2})	I_a	$r_{eo} = R_{ne} / R_n$	Z-test
Model 1	1,200	26	21	1.00	1.02	F
Model 2	1,200	26	20	1.00	1.02	F
Model 3	1,200	39	31	1.00	1.06	F
Daily comparison	**Number of observations**	**RMSE (MJ m^{-2} d^{-1})**	**MAE (MJ m^{-2} d^{-1})**	**I_a**	**$r_{eo} = R_{ne} / R_n$**	**Z-test**
Model 1	25	1.29	1.09	0.93	1.03	F
Model 2	25	1.22	1.04	0.96	1.02	F
Model 3	25	1.54	1.35	0.94	1.03	F

RMSE = root mean square error; MAE = mean absolute error; I_a = index of agreement; r_{eo} = ratio of estimated (R_{ne}) to observed (R_n) values of net radiation on 30-min and daily basis; T = true hypothesis ($b = 1$); F = false hypothesis ($b \neq 1$).

Table 3. Examples of several empirical and semi-empirical methods used to estimate the net radiation (R_n) for different type of vegetation.

Authors	Location	Vegetation	General equation used	Number	Suppositions and principal calculations
Ortega-Farías et al. (2000)	Avignon, France and Talca, Chile	Grass at reference condition	$R_n = (1-\alpha)R^{\downarrow}+(\varepsilon_a\sigma T_a^4 - \varepsilon_{cv}\sigma T_{cv}^4)$	12	$\varepsilon_a = 1.31(e_a/T_a)^{1/7}$ $\alpha = 0.25$
Irmak et al. (2003)	Florida; Georgia; Utah; Texas, USA	Fescue grass	$R_n = (1-\alpha)R^{\downarrow}+(R_l^{\downarrow} - R_l^{\uparrow})$ $R_n = (1-\alpha)R^{\downarrow}+R_l$	13	$R_l = \sigma[(T_{max}^4 + T_{min}^4)/2](0.34 - 0.14(e_a)^{1/2}[1.35(R^{\downarrow}/R^{\downarrow}_{clear\text{-}sky}) - 0.35]$ $\alpha = 0.23$
			$R_n = (-0.054T_{max}) + (0.111T_{min}) + (0.462R^{\downarrow}) + (-49.243d_r) + 50.831$	14	$d_r = 1 + 0.033\cos[(2\pi/365)JD]$ $JD = DOY$
Samani et al. (2007)	Chamberino and Socorro, New Mexico	Pecan tree; Salcedar tree; Cottonwood tree	$R_n = R_{ni}[(R^{\downarrow}/R_i^{\downarrow})(T_{avg}/T_a)^4]$ $R_{ni} = (1-\alpha)R^{\downarrow}+\varepsilon_a\sigma T_a^4 - \varepsilon_s\sigma T_s^4 - (1 - \varepsilon_s)\varepsilon_a\sigma T_a^4$	15	*Method "a" calculates R_n using ground measurement; R_s, R_{ni}, R_{si}, T_{avg} and T_a* $T_{avg} = (T_{max} + T_{min})/2$
Carrasco and Ortega-Farías (2008)	Región del Maule, Chile	Vineyard	$R_n = (1-\alpha)R^{\downarrow}+(\varepsilon_a\sigma T_a^4 - \varepsilon_{cv}\sigma T_{cv}^4)$	16	$T_{cv} = T_s$ $\varepsilon_a = 1.51(e_a/T_a)^{1/7}(R^{\downarrow} > 0)$ $\varepsilon_a = 1.91(e_a/T_a)^{1/7}(R^{\downarrow} < 0)$ $\alpha = 0.18$
Sentelhas and Gillespie (2008)	Ontario, Canada	Turfgrass	$R_n = 0.837(0.77R^{\downarrow}) – 0.0275[5.67x10^{-8}(273 + T_a^4)] – 37.7$	17	$\alpha = 0.23$ *Average empirical coefficient obtained by Iziomon et al (2000) was used*
Berni et al. (2009)	Southern, Spain	Olive orchard	$R_n = (1-\alpha)R^{\downarrow}+\varepsilon_s R_l^{\downarrow} - \varepsilon_s\sigma T_s^4$	18	$R_l^{\downarrow} = [clf + (1 - clf)\varepsilon_a]\sigma T_a^4$ ε_a *in fuction of* e_a *and* T_a
Ezzahar et al. (2009)	Niamey, Niger	Shrubs	$R_n = (1-\alpha)R^{\downarrow}+\varepsilon_s R_l^{\downarrow} - \varepsilon_s \sigma T_s^4$	19	$\varepsilon_a = 1.24(e_a/T_a)^{1/7}$

Table 3. Continued.

Authors	Location	Vegetation	General equation used	Number	Suppositions and principal calculations
Kjaersgaard et al. (2009)	Taastrup and Foulum, Denmark	Green grass	$R_n = (1-\alpha)R^{\downarrow}+(R_l^{\downarrow} - R_l^{\uparrow})$ $R_n = (1-\alpha)R^{\downarrow}+R_l$	20	$R_l = \sigma[(T_{max}^4 + T_{min}^4)/2]$ $(0.34 - 0.14(e_a)^{1/2}[1.35(R^{\downarrow}/R^{\downarrow}_{clear\text{-}sky}) - 0.35]$ $\alpha = 0.25$
	Zaragoza and Córdoba, Spain	Green grass			
Irmak et al. (2010)	Nebraska and California, USA	Maize crop	$R_n = (1-\alpha)R^{\downarrow}+(R_l^{\downarrow} - R_l^{\uparrow})$ $R_n = (1-\alpha)R^{\downarrow}+R_l$	21	$R_l = \sigma[(T_{max}^4 + T_{min}^4)/2]$ $(0.34 - 0.14(e_a)^{1/2}[1.35(R^{\downarrow}/R^{\downarrow}_{clear\text{-}sky}) - 0.35]$ $R^{\downarrow}_{clear\text{-}sky} = R_a^{\downarrow}\tau_{sw}$ $\tau_{sw} = 0.75 + 2x10^{-5}(z)$ $\alpha = 0.19$
Ortega-Farías et al. (2010)	Región del Maule, Chile	Vineyard	$R_n = (1-\alpha)R^{\downarrow}+(\varepsilon_a\sigma T_a^4 - \varepsilon_s\sigma T_s^4)$	22	$T_s \approx (f_c T_{cv}^4 + (1 - f_c)T_{soil}^4)^{1/4}$ $\varepsilon_a = 1.51(e_a/T_a)^{1/7}(R^{\downarrow} > 0)$ $\varepsilon_a = 1.91(e_a/T_a)^{1/7}(R^{\downarrow} < 0)$ $\alpha = 0.19$

clf: cloud fraction term; d_r: inverse relative earth–sun distance; z: elevation; e_a: air vapor pressure; *JD or DOY*: day of the year or Julian day; f_c: fractional cover; T_a, T_{avg}, T_s, T_{cv} and T_{soil}: air, average, surface, canopy and soil temperatures; T_{max} and T_{min}: maximum and minimum air temperatures; τ_{sw}: atmospheric transmissivity from elevation; α: albedo; σ: Stefan–Boltzmann constant; ε_a and ε_s: air and surface emissivity; $R^{\downarrow}$ and $R_l^{\downarrow}$: incoming short and long wave radiation; $R_l^{\uparrow}$: outgoing long wave radiation; R_l: outgoing net long wave radiation; $R^{\downarrow}_{clear\text{-}sky}$: clear-sky short wave radiation; R_{ni}: incident (instantaneous) net radiation; $R_i^{\downarrow}$: incident incoming short wave radiation; $R_a^{\downarrow}$: extraterrestrial radiation.

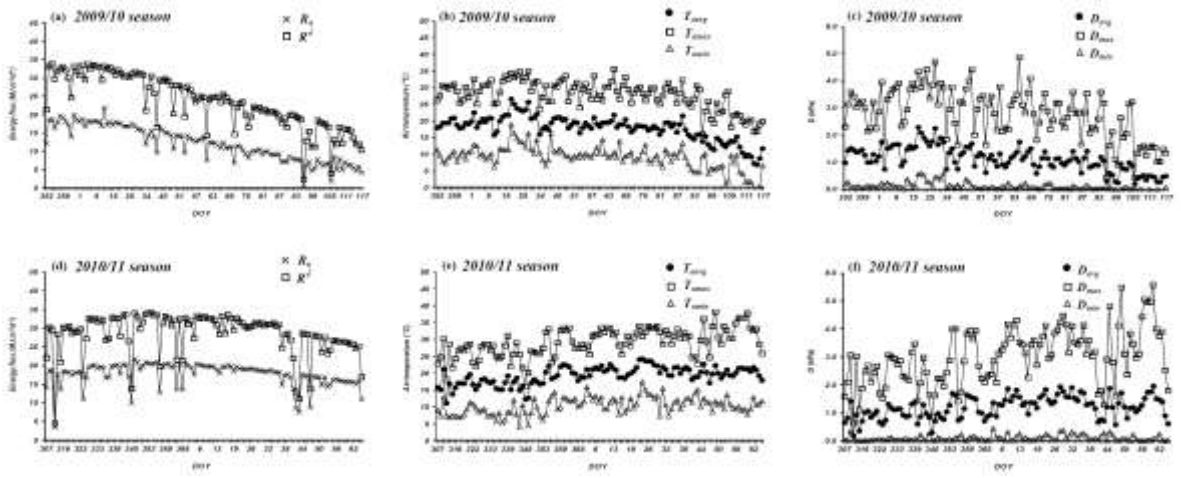

Figure 1. Daily values of [(a) and (d)] incoming short wave radiation ($R_s^{\downarrow}$), net radiation (R_n); [(b) and (e)] air temperature (T_a); and [(c) and (f)] vapour pressure deficit (D) during the 2009/10 and 2010/11 seasons, respectively.

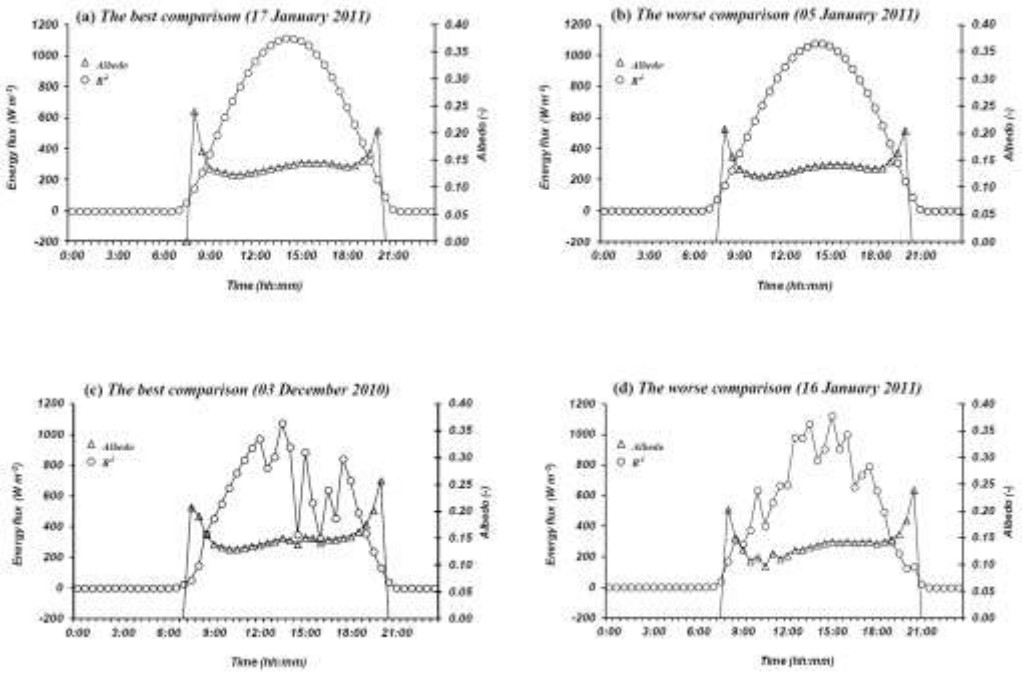

Figure 2. Daytime variation of the best [(a) and (c)] and worse [(b) and (d)] comparison of the incoming short wave radiation ($R_s^{\downarrow}$) and albedo for the representative clear days during 2009/10 and 2010/11 seasons.

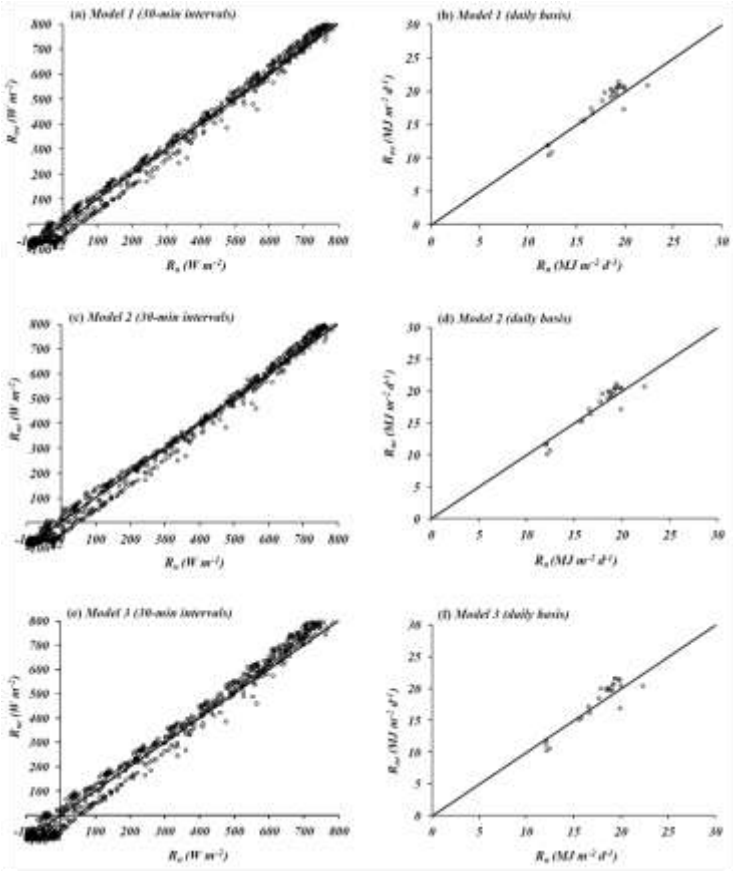

Figure 3. Comparisons between estimated (R_{ne}) and observed (R_n) net radiation at 30-min interval [(a), (c) and (e)] and daily basis [(b), (d) and (f)] using *Model 1*, *2* and *3* for validation season. The solid line represents the 1:1 line.

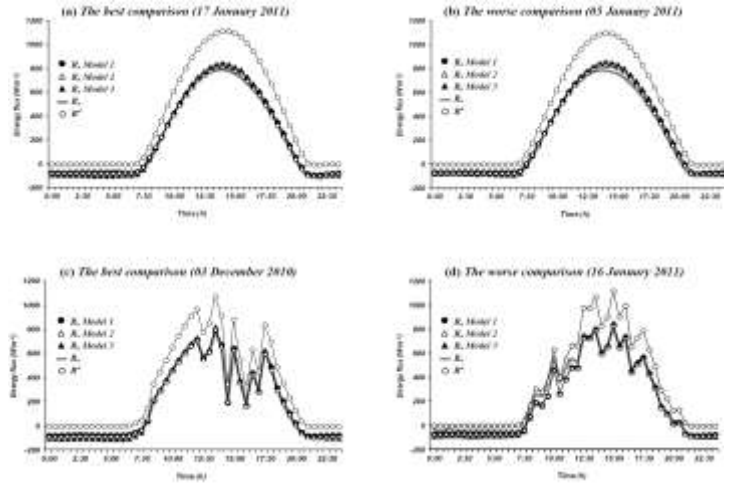

Figure 4. The best [(a) and (c)] and worse [(b) and (d)] comparison between observed (R_n) and estimated (R_{ne}) values of net radiation for the *Models 1*, *2* and *3* under clear and cloudy days for validation season. The incoming short wave radiation ($R^{\downarrow}$) is included as a reference.